

# CONTROL OF OSCILLATIONS IN TWO-ROTOR CYBERPHYSICAL VIBRATION UNITS WITH TIME-VARYING OBSERVER

**Olga P. Tomchina**

Saint Petersburg State University of Architecture and Civil Engineering (SPSUACE),  
2-nd Krasnoarmeiskaya St. 4, 190005, St. Petersburg, Russian Federation  
otomchina@mail.ru

Article history:

Received 12.12.2020, Accepted 25.12.2020

## Abstract

In this paper the control of oscillations in the two-rotor vibration unit is studied. It is assumed that the velocity of the oscillation of the platform cannot be accurately measured. The time-varying observer is proposed to restore it. In order to guarantee stability of the frequency and amplitude of oscillations of the vibrating parts of a two-rotor vibration unit special control algorithms based on speed-gradient methodology. Simulation results confirm stability of the synchronous rotation modes of the unbalanced rotors of the vibration unit.

## 1 Introduction

A promising direction in cybernetical physics is investigation of possible changes of complex nonlinear systems oscillatory behavior under bounded control. A series of benchmark examples are provided by vibration units. The case of 1DOF system models (pendulum or vibroactuator) is well studied [Andrievskii et al., 2001; Fradkov, 1999], as well as the case of synchronization for two or more 1DOF systems [Blekhman et al., 2002]. However for multi-DOF systems, like multirotor vibration actuator a number of problems need further study [Efimov et al., 2013].

The design of controllers for complex mechanical system is usually performed under assumption that all the state variables are available for measurement. However this assumption usually does not hold for experimental study since measurement of the signal derivatives is usually made with low accuracy. To overcome the incompleteness of the measurements the observers or filters are used. For the vibration units with one-DOF supporting body such a study was performed [Fradkov et al., 2016].

In this paper the case of the two-rotor vibration unit is studied. In such a unit the measurement of the oscillation of the platform cannot be accurately measured and

the time-varying observer is used to restore it. In order to guarantee stability of the frequency and amplitude of oscillations of the vibrating parts of a two-rotor vibration unit special algorithms for controlling the synchronous rotation modes of unbalanced rotors are used. An efficient method for design of the control algorithms is the speed gradient method allowing to deal with strongly nonlinear systems [Fradkov et al., 1999]. The installation of all required sensors for such a complex interconnected system as a two-rotor vibrator that vibrates in the vertical plane is impossible because of unfavorable operating factors, e.g. the dustiness when processing bulk materials, or a significant increase in the amplitude of vibrations during passing through the resonance zone. In addition, as the number of sensors increases, reliability of the system decreases and the unit costs increases. Many existing sensors do not admit processing information in real time due to the limitations of the communication channels between the unit and the controlling computer. It leads to the decrease of the speed of information exchange and decrease of the system performance. A promising way to overcome the difficulties associated with processing information from sensors in the control system is using state observers instead of some sensors. It allows one to provide estimates of the missing variables based on the results of measurements using the available sensors. Such an approach is in accordance with the current trend in the control technology called "sensorless control" [Lascu et al., 2000; Wang et al., 2019; Bobtsov et al., 2018; Ortega et al., 2019]. In the works on sensorless control the information about the angular speed of the motors is estimated from the results of measurements obtained with the help of stator voltage and current sensors. In [Lascu et al., 2000] a method for controlling the torque of an induction motor is proposed, which is based not on information from sensors, but on estimates of the magnitude of the flow and torque.

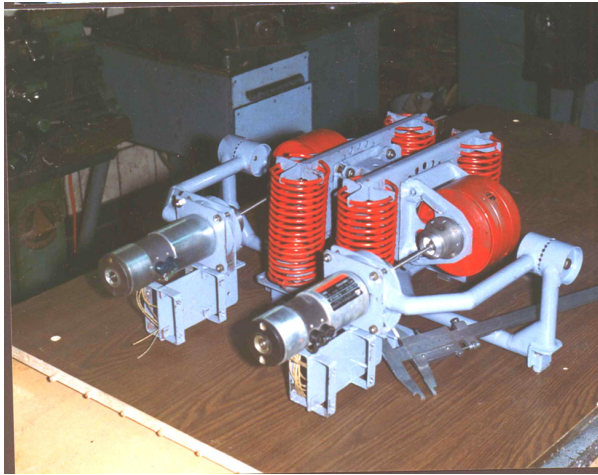


Figure 1. Vibration unit SV-1.

A review of works on the control of drive systems with permanent magnet synchronous motors with incomplete measurement of the vector of variables required to generate a control signal is presented in [Wang et al., 2019]. The other works are devoted to the synthesis of observers to control the systems of magnetic levitation [Bobtsov et al., 2018], sensorless control of switched jet engines [Ortega et al., 2019] etc. In the work [Fradkov et al., 2016] a non-stationary observer was synthesized for a single-rotor vibratory unit, which restored information about the vertical speed of the platform and made it possible to implement an algorithm for passing through the resonant frequency, which was also developed on the basis of the speed gradient method.

In this paper, we consider the possibility of implementing a rotor synchronization control algorithm using an observer restoring the vertical speed of the platform for a two-rotor vibration installation. The synthesis of the observer is performed according to a simplified model of the dynamics of a two-rotor VU, which describes the movement of the installation along the vertical axis  $Oy$ . The performance of the synthesized observer is assessed using computer simulation in the MATLAB environment for a more detailed model of the dynamics of a two-rotor VU, which describes the vibrations of the installation in the vertical plane. In addition, the model takes into account the influence of the dynamics of the system of electric drives of unbalanced rotors.

## 2 Model of Two-rotor Vibration Unit Taking into Account the Drive Dynamics

In this section the mathematical model of the vibration unit and the control algorithm are described following [Tomchina, 2018]. Besides, the drive dynamics model, schematics of the SV-1 vibration unit (Fig. 1) and the nomenclature of the variables (Fig. 2) are presented, following [Tomchina, 2019].

In Fig. 2  $\varphi, \varphi_1, \varphi_2$  are angle of the supporting body and rotation angles of the rotors, respectively, measured from the horizontal position,  $x_c, y_c$  are the horizontal and vertical displacement of the supporting body from the equilibrium position,  $m_i = m, i = 1, 2$  and  $m_n$  are the masses of the rotors and supporting body,  $J_1, J_2$  are the inertia moments of the rotors,  $\varrho_1 = \varrho, i = 1, 2$  are the rotor eccentricities,  $c_{01}, c_{02}$  are the horizontal and vertical spring stiffness,  $g$  is the gravity acceleration,  $m_0$  is the total mass of the unit,  $m_0 = 2m + m_n$ ,  $\beta$  is the damping coefficient,  $k_c$  is the friction coefficient in the bearings,  $M_i$  are the motor torques (controlling variables). It is assumed that rotor shafts are orthogonal to the motion of the support.

To convert the scheme into the state space equations, assume that the whole system dynamics may be considered in the vertical plane. Then the equations of dynamics have the following form [Tomchina et al., 2015]:

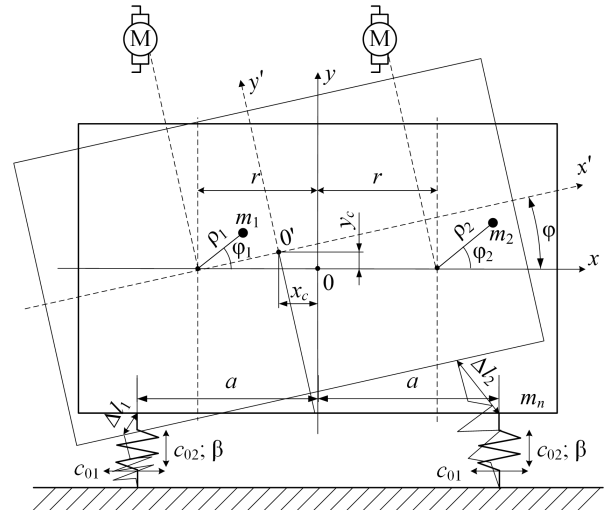


Figure 2. Schematics of two-rotor vibration unit with DC motors.

$$\begin{aligned}
& m_0 \ddot{x}_c - \ddot{\varphi} m \varrho (\sin(\varphi + \varphi_1) + \sin(\varphi + \varphi_2)) - \\
& \ddot{\varphi}_1 m \varrho \sin(\varphi + \varphi_1) - \ddot{\varphi}_2 m \varrho \sin(\varphi + \varphi_2) - \\
& \dot{\varphi}^2 m \varrho (\cos(\varphi + \varphi_1) + \cos(\varphi + \varphi_2)) - \\
& \dot{\varphi}_1^2 m \varrho \cos(\varphi + \varphi_1) - \dot{\varphi}_2^2 m \varrho \cos(\varphi + \varphi_2) - \\
& 2\dot{\varphi} \dot{\varphi}_1 m \varrho \cos(\varphi + \varphi_1) - \\
& 2\dot{\varphi} \dot{\varphi}_2 m \varrho \cos(\varphi + \varphi_2) + 2c_{01} x_c + \beta \dot{x}_c = 0; \\
& m_0 \ddot{y}_c + \ddot{\varphi} m \varrho (\cos(\varphi + \varphi_1) + \cos(\varphi + \varphi_2)) + \\
& \ddot{\varphi}_1 m \varrho \cos(\varphi + \varphi_1) + \ddot{\varphi}_2 m \varrho \cos(\varphi + \varphi_2) - \\
& \dot{\varphi}^2 m \varrho (\sin(\varphi + \varphi_1) + \sin(\varphi + \varphi_2)) - \\
& \dot{\varphi}_1^2 m \varrho \sin(\varphi + \varphi_1) - \dot{\varphi}_2^2 m \varrho \sin(\varphi + \varphi_2) - \\
& 2\dot{\varphi} \dot{\varphi}_1 m \varrho \sin(\varphi + \varphi_1) - 2\dot{\varphi} \dot{\varphi}_2 m \varrho \sin(\varphi + \varphi_2) + \\
& m_0 g + 2c_{02} y_c + \beta \dot{y}_c = 0; \\
& -\ddot{x}_c m \varrho (\sin(\varphi + \varphi_1) + \sin(\varphi + \varphi_2)) + \\
& \ddot{y}_c m \varrho (\cos(\varphi + \varphi_1) + \cos(\varphi + \varphi_2)) + \\
& \ddot{\varphi} (J + J_1 + J_2 - 2m \varrho r (\cos \varphi_1 - \cos \varphi_2)) + \\
& \ddot{\varphi}_1 (J_1 - m \varrho r \cos \varphi_1) + \ddot{\varphi}_2 (J_2 + m \varrho r \cos \varphi_2) + \\
& \dot{\varphi}_1^2 m \varrho r \sin \varphi_1 - \dot{\varphi}_2^2 m \varrho r \sin \varphi_2 + 2m \varrho r \dot{\varphi} \dot{\varphi}_1 \sin \varphi_1 - \\
& 2m \varrho r \dot{\varphi} \dot{\varphi}_2 \sin \varphi_2 + m \varrho g (\cos(\varphi + \varphi_1) + \\
& \cos(\varphi + \varphi_2)) + c_{03} \varphi + \beta \dot{\varphi} = 0; \\
& -\ddot{x}_c m \varrho \sin(\varphi + \varphi_1) + \ddot{y}_c m \varrho \cos(\varphi + \varphi_1) + \\
& \ddot{\varphi} (J_1 - m \varrho r \cos \varphi_1) + \ddot{\varphi}_1 J_1 - \dot{\varphi}^2 m \varrho r \sin \varphi_1 + \\
& m \varrho g \cos(\varphi + \varphi_1) + k_r \dot{\varphi}_1 = M_{m1}; \\
& -\ddot{x}_c m \varrho \sin(\varphi + \varphi_2) + \ddot{y}_c m \varrho \cos(\varphi + \varphi_2) + \\
& \ddot{\varphi} (J_2 + m \varrho r \cos \varphi_2) + \ddot{\varphi}_2 J_2 + \dot{\varphi}^2 m \varrho r \sin \varphi_2 + \\
& m \varrho g \cos(\varphi + \varphi_2) + k_r \dot{\varphi}_2 = M_{m2};
\end{aligned} \tag{1}$$

When taking into account the dynamics of the drive in the simulation process the control torque  $M_{m1}$  arriving at the input of the "unbalanced rotor" is formed in accordance with the structural diagram of the "electric drive". Since the laboratory setup SV-1 used the DC motors, the electric drive structure is selected as the traditional system with current loop. The proportional-integral (PI) current controller  $W_{CR}(p) = b(\tau p + 1)/\tau p$  is configured to optimum modulo;  $b$ ,  $\tau$  are dynamic gain and time constant of the regulator. The following notation is used here: CR is the current regulator; TC is the power (thyristor type) converter; CS is the current sensor;  $I_a$  is the armature current;  $E_{TC}$  and  $E_m$  are converter and motor EMFs;  $k_{TC}$  and  $k_{CS}$  are converter and current feedback gains;  $kF$  is the motor torque (EMF) coefficient;  $T_{TC}$  and  $T_{CS}$  are converter and current sensor time constants;  $T_a$  is the armature time constant;  $R_a$  is the armature circuit resistance;  $U_{CR}$  and  $U_{CS}$  are current controller and current sensor output voltages;  $U_i$  is the voltage corresponding to the calculated torque  $M_{mi}$ , obtained in accordance with the equations (1),  $k_m = kF$ .

In accordance with [Tomchina, 2019] the drive dynamics are described as follows

$$\begin{aligned}
\dot{I}_a &= \frac{1}{T_a} \left( -I_a + \frac{1}{R_a} (E_{TC} - E_m) \right), \\
\dot{E}_{TC} &= \frac{1}{T_{TC}} (-E_{TC} + k_{TC} U_{CR}), \\
\dot{U}_{CS} &= \frac{1}{T_{CS}} (-U_{CS} + k_{CS} I_a), \\
\dot{U}_{CS1} &= \frac{b}{\tau} (U_1 - U_{CS}), \\
U_{CS} &= b(U_1 - U_{CS}) + U_{CS1}, \\
E_m &= kF \dot{\varphi}, \quad M_m = k_M I_a
\end{aligned} \tag{2}$$

### 3 Integral-Differential Speed-Gradient Control Algorithms for Synchronization of Two-Rotor Vibration Unit

Frequency synchronization is defined as an exact coincidence of angular velocities of the unbalanced rotors  $\omega_s = \omega_r$ ;  $s, r = 1, \dots, k$ . [Blekhman, 2000]. For practice approximate synchronization conditions are more appropriate [Tomchina et al., 2015]:

$$|\omega_s - \omega_r| \leq \varepsilon. \tag{3}$$

where  $\varepsilon > 0$  can be chosen numerically as  $\varepsilon = 0,05\omega^*$ . However the relation (3) may be not sufficient for synchronization, since its fulfillment does not prevent the accumulation of the error in phase (phase shift). That is why there is a need to impose additional requirements on the system phases. To this end the notion of approximate phase synchronization is formulated as follows [Tomchina et al., 2015]:

$$|\varphi_s - \varphi_r - L_{sr}| < \varepsilon; \quad s, r = 1, \dots, k. \tag{4}$$

Equations (3) and (4) should hold for some  $\varepsilon > 0$ , and some real  $L_{sr}$ .

To provide a synchronous rotation mode of unbalanced rotors for system (1), it is suggested to use speed-gradient method with an objective functional in the following form:

$$Q(z) = \left\{ 0.5(1 - \alpha)(H - H^*)^2 + \alpha(\dot{\varphi}_1 \pm \dot{\varphi}_2)^2 \right\}, \tag{5}$$

where  $z = [x_c, \dot{x}_c, y_c, \dot{y}_c, \varphi, \dot{\varphi}, \varphi_1, \dot{\varphi}_1, \varphi_2, \dot{\varphi}_2]^T$ ,  $0 < \alpha < 1$  is weight coefficient;  $H$  is total mechanical energy of a system (1),  $H^*$  is the desired value of  $H$ .

If the value of the objective functional (5) satisfies  $Q(z) = 0$ , then the energy achieves the prespecified value:  $H = H^*$  and the rotor velocities are equal:  $\dot{\varphi}_1 = \dot{\varphi}_2$ .

The proportional-integral (PI-) speed-gradient algorithm in the finite form with the objective functional (5) is as follows [Tomchina, 2019]:

$$\begin{aligned}
M_1 &= -\gamma_1 \left\{ (1 - \alpha)(H - H^*) \dot{\varphi}_1 + \right. \\
&\quad \left. \frac{\alpha}{J_1} (\dot{\varphi}_1 \pm \dot{\varphi}_2) + \frac{\alpha}{J_1} (\varphi_1 \pm \varphi_2 + \Delta \varphi_1) \right\}. \tag{6}
\end{aligned}$$

Total mechanical energy of a system (1) is  $H = T + \Pi$ , where kinetic and potential energies  $T$  and  $\Pi$  are as follows:

$$\begin{aligned} T &= 0.5m_0 (\dot{x}_c^2 + \dot{y}_c^2) + 0.5\dot{\varphi}^2 (J + J_1 + J_2 - \\ & 2dm_\varrho (\cos \varphi_1 - \cos \varphi_2)) + 0.5J_1\dot{\varphi}_1^2 + 0.5J_2\dot{\varphi}_2^2 + \\ & \dot{\varphi}\dot{\varphi}_1 (J_1 - dm_\varrho \cos \varphi_1) + \dot{\varphi}\dot{\varphi}_2 (J_2 + dm_\varrho \cos \varphi_2) - \\ & \dot{x}_c\dot{\varphi}m_\varrho (\sin (\varphi + \varphi_1) + \sin (\varphi + \varphi_2)) + \\ & \dot{y}_c\dot{\varphi}m_\varrho (\cos (\varphi + \varphi_1) + \cos (\varphi + \varphi_2)) - \\ & \dot{x}_c\dot{\varphi}_1m_\varrho \sin (\varphi + \varphi_1) + \dot{y}_c\dot{\varphi}_1m_\varrho \cos (\varphi + \varphi_1) - \\ & \dot{x}_c\dot{\varphi}_2m_\varrho \sin (\varphi + \varphi_2) + \dot{y}_c\dot{\varphi}_2m_\varrho \cos (\varphi + \varphi_2), \\ \Pi &= m_0gy_c + m_\varrho g (\sin (\varphi + \varphi_1) + \sin (\varphi + \varphi_2)) + \\ & c_{01} (x_c^2 + \alpha^2 \cos^2 \varphi)^2 + c_{02} (y_c^2 + \alpha^2 \sin^2 \varphi), \end{aligned}$$

Then we simplify the expression for the total mechanical energy  $H$  in order to exclude the variables that cannot be measured by existing sensors and are sufficiently small to be neglected. In [Fradkov et al., 2013] the possibility of effective control was shown in the absence of information about the platform rotation angle  $\varphi$ . Therefore, it is permissible to simplify the expression for the total energy by setting  $\varphi = 0$ . In addition the horizontal movements of the platform  $x_c$  are neglectable too. However, the speed of vertical movements  $\dot{y}_c$  cannot be ignored and will be restored by the observer. To justify such a simplification a series of computer simulations will be performed.

#### 4 Design of the Observer for Velocity of the Vibration Unit Moving Along the Vertical Axis

As is seen from (6), the current value of the mechanical energy of the system  $H(t)$  is required to compute control signal  $M(t)$ . The inductive position sensors are used to measure the supporting body coordinates  $y_c$ . However supporting body velocity  $\dot{y}_c$  cannot be measured. Therefore we estimate it using a time-varying observer as follows.

For the observer design we use the simplified model where neither horizontal movements of the platform  $x_c$  nor the platform rotation angle  $\varphi$  are taken into account:

$$\begin{aligned} m_0\ddot{y}_c + m_\varrho \sin \varphi_1 \ddot{\varphi}_1 + m_\varrho \sin \varphi_2 \ddot{\varphi}_2 + m_\varrho \cos \varphi_1 \dot{\varphi}_1^2 + \\ m_\varrho \cos \varphi_2 \dot{\varphi}_2^2 + m_0g + 2c_0y_c + \beta\dot{y}_c &= 0; \\ m_\varrho \sin \varphi_1 \ddot{y}_c + J_1\ddot{\varphi}_1 + m_\varrho g \sin \varphi_1 + k_c \cdot \dot{\varphi}_1 &= M_1; \\ m_\varrho \sin \varphi_2 \ddot{y}_c + J_2\ddot{\varphi}_2 + m_\varrho g \sin \varphi_2 + k_c \cdot \dot{\varphi}_2 &= M_2; \end{aligned} \quad (7)$$

We represent the first of equation in (7) as follows:

$$m_0\ddot{y}_c + \beta\dot{y}_c + 2c_0y_c = F(t), \quad (8)$$

where

$$F(t) = -m_\varrho \sin \varphi_1 \ddot{\varphi}_1 - m_\varrho \cos \varphi_1 \dot{\varphi}_1^2 - \\ m_\varrho \sin \varphi_2 \ddot{\varphi}_2 - m_\varrho \cos \varphi_2 \dot{\varphi}_2^2 - m_0g. \quad (9)$$

Resolve the system (7) with respect to the highest

derivatives:

$$\begin{aligned} \ddot{y}_c &= -\frac{J_1J_2(m_\varrho \cos \varphi_1 \dot{\varphi}_1^2 + m_\varrho \cos \varphi_2 \dot{\varphi}_2^2 + m_0g + 2c_0y_c + \beta\dot{y}_c)}{\Delta(t)} - \\ & \frac{J_1m_\varrho \sin^2 \varphi_2 (M_2 - k_c \dot{\varphi}_2 - m_\varrho g \sin \varphi_2)}{\Delta(t)} + \\ & \frac{J_2m_\varrho \sin^2 \varphi_1 (M_1 - k_c \dot{\varphi}_1 - m_\varrho g \sin \varphi_1)}{\Delta(t)}; \\ \ddot{\varphi}_1 &= \frac{(m_0J_2 - m^2\varrho^2 \sin^2 \varphi_2)(M_1 - k_c \dot{\varphi}_1 - m_\varrho g \sin \varphi_1)}{\Delta(t)} + \\ & \frac{m^2\varrho^2 \sin \varphi_1 \sin \varphi_2 (M_2 - k_c \dot{\varphi}_2 - m_\varrho g \sin \varphi_2)}{\Delta(t)} + \\ & \frac{J_2m_\varrho \sin \varphi_1 (m_\varrho \cos \varphi_1 \dot{\varphi}_1^2 + m_\varrho \cos \varphi_2 \dot{\varphi}_2^2 + m_0g + 2c_0y_c + \beta\dot{y}_c)}{\Delta(t)}; \\ \ddot{\varphi}_2 &= \frac{(m_0J_1 - m^2\varrho^2 \sin^2 \varphi_1)(M_2 - k_c \dot{\varphi}_2 - m_\varrho g \sin \varphi_2)}{\Delta(t)} + \\ & \frac{m^2\varrho^2 \sin \varphi_1 \sin \varphi_2 (M_1 - k_c \dot{\varphi}_1 - m_\varrho g \sin \varphi_1)}{\Delta(t)} + \\ & \frac{J_1m_\varrho \sin \varphi_2 (m_\varrho \cos \varphi_1 \dot{\varphi}_1^2 + m_\varrho \cos \varphi_2 \dot{\varphi}_2^2 + m_0g + 2c_0y_c + \beta\dot{y}_c)}{\Delta(t)}; \end{aligned}$$

where  $\Delta(t) = M_0J_1J_2 - J_1m^2\varrho^2 \sin^2 \varphi_2 - J_2m^2\varrho^2 \sin^2 \varphi_1$ .

Substitute  $\ddot{\varphi}_1, \ddot{\varphi}_2$  into the expression (8) for  $F(t)$ :

$$\begin{aligned} F(t) &= -\frac{m_\varrho \sin \varphi_1}{\Delta(t)} \{ (m_0J_2 - m^2\varrho^2 \sin^2 \varphi_2) \times \\ & \times [M_1 - k_c \dot{\varphi}_1 - m_\varrho g \sin \varphi_1] + J_2m_\varrho \sin \varphi_1 \times \\ & (m_\varrho \cos \varphi_1 \dot{\varphi}_1^2 + m_\varrho \cos \varphi_2 \dot{\varphi}_2^2 + m_0g + 2c_0y_c + \beta\dot{y}_c) + \\ & m^2\varrho^2 \sin \varphi_1 \sin \varphi_2 [M_2 - k_c \dot{\varphi}_2 - m_\varrho g \sin \varphi_2] \} - \\ & m_\varrho \cos \varphi_1 \dot{\varphi}_1^2 - m_\varrho \cos \varphi_2 \dot{\varphi}_2^2 - m_0g - \frac{m_\varrho \sin \varphi_2}{\Delta(t)} \times \\ & \{ (m_0J_1 - m^2\varrho^2 \sin^2 \varphi_1) [M_2 - k_c \dot{\varphi}_2 - m_\varrho g \sin \varphi_2] + \\ & m^2\varrho^2 \sin \varphi_1 \sin \varphi_2 [M_2 - k_c \dot{\varphi}_1 - m_\varrho g \sin \varphi_1] + \\ & J_1m_\varrho \sin \varphi_2 [m_\varrho \cos \varphi_1 \dot{\varphi}_1^2 + m_\varrho \cos \varphi_2 \dot{\varphi}_2^2 + \\ & m_0g + 2c_0y_c + \beta\dot{y}_c] \}. \end{aligned} \quad (10)$$

Moving the terms  $\left(\frac{-J_2m^2\varrho^2 \sin^2 \varphi_1}{\Delta(t)}\right)\beta\dot{y}_c$  and  $\left(\frac{-J_1m^2\varrho^2 \sin^2 \varphi_2}{\Delta(t)}\right)\beta\dot{y}_c$  into the left-hand side of equation (8) we obtain

$$m_0\ddot{y}_c + \beta \left( 1 + \frac{J_2m^2\varrho^2 \sin^2 \varphi_1 + J_1m^2\varrho^2 \sin^2 \varphi_2}{\Delta(t)} \right) \dot{y}_c + \\ + 2c_0y_c = F_1(t), \quad (11)$$

where the function  $F_1(t)$  is as follows:

$$F_1(t) = F(t) + \frac{J_2m^2\varrho^2 \sin^2 \varphi_1 + J_1m^2\varrho^2 \sin^2 \varphi_2}{\Delta(t)} \beta\dot{y}_c.$$

It is seen that the expression for  $F_1(t)$  does not contain the terms with  $\dot{y}_c$  since they are annihilated.

Note that  $F_1(t)$  depends only on variables measured by sensors  $[y_c, \varphi_1, \dot{\varphi}_1, \varphi_2, \dot{\varphi}_2]^T$ .

Convert the expression in parentheses in (11)

$$1 + \frac{J_2m^2\varrho^2 \sin^2 \varphi_1 + J_1m^2\varrho^2 \sin^2 \varphi_2}{m_0J_1J_2 - J_1m^2\varrho^2 \sin^2 \varphi_2 - J_2m^2\varrho^2 \sin^2 \varphi_1} = \\ = \frac{m_0J_1J_2}{m_0J_1J_2 - J_1m^2\varrho^2 \sin^2 \varphi_2 - J_2m^2\varrho^2 \sin^2 \varphi_1} = \frac{m_0J_1J_2}{\Delta(t)}.$$

Introduce the coefficient  $\beta_1(t)$

$$\beta_1(t) = \beta \left( \frac{m_0J_1J_2}{m_0J_1J_2 - J_1m^2\varrho^2 \sin^2 \varphi_2 - J_2m^2\varrho^2 \sin^2 \varphi_1} \right) = \\ = \beta \frac{m_0J_1J_2}{\Delta(t)}.$$

It is obvious that  $\max \Delta(t) = \max (m_0 J_1 J_2 - J_1 m^2 \varrho^2 \sin^2 \varphi_2 - J_2 m^2 \varrho^2 \sin^2 \varphi_1) = m_0 J_1 J_2$ , because  $J_1, J_2, m, \varrho, m_0$  are positive values, since these are the mass-inertial parameters of the installation. Then  $\min \frac{m_0 J_1 J_2}{\Delta(t)} = 1$  and coefficient  $\beta_1(t) \geq \beta$ .

Therefore, (11) takes the form

$$m_0 \ddot{y}_c + \beta_1(t) \dot{y}_c + 2c_0 y_c = F_1(t). \quad (12)$$

This equation is linear and non-stationary.

We proceed from the second order differential equation (12) to the state equations, denoting  $x_1 = y_c, x_2 = \dot{y}_c$ .

$$\begin{cases} \dot{x}_1(t) = x_2; \\ \dot{x}_2(t) = -\beta_0(t)x_2(t) - c'_0 x_1(t) + F_2(t), \end{cases} \quad (13)$$

where  $\beta_0(t) = \beta_1(t)/m_0$ ;  $c_0 = 2c_0/m_0$ ;  $F_2(t) = F_1(t)/m_0$ ,

The non-stationary unit equations (13) can be written in vector-matrix form:

$$\begin{pmatrix} \dot{x}_1 \\ \dot{x}_2 \end{pmatrix} = \begin{pmatrix} 0 & 1 \\ -c'_0 & -\beta_0(t) \end{pmatrix} \cdot \begin{pmatrix} x_1 \\ x_2 \end{pmatrix} + \begin{pmatrix} 0 \\ F_2(t) \end{pmatrix}. \quad (14)$$

Then the equations of the non-stationary observer of complete order are written in the form:

$$\begin{cases} \dot{\hat{x}}_1(t) = \hat{x}_2(t) + k_1(x_1(t) - \hat{x}_1(t)); \\ \dot{\hat{x}}_2(t) = -\beta_0(t)\hat{x}_2(t) - c'_0\hat{x}_1(t) + F_2(t) + \\ + k_2(x_1(t) - \hat{x}_1(t)), \end{cases} \quad (15)$$

where  $x_1(t)$  is measured by sensors.

Then the differential equations for the observation errors  $e_{N1}(t) = x_1(t) - \hat{x}_1(t)$ ,  $e_{N2}(t) = x_2(t) - \hat{x}_2(t)$ , are as follows:

$$\begin{aligned} \dot{e}_{N1}(t) &= x_2(t) - \hat{x}_2(t) - k_1(x_1(t) - \hat{x}_1(t)) = \\ &= e_{N2}(t) - k_1 e_{N1}(t); \\ \dot{e}_{N2}(t) &= \dot{x}_2(t) - \dot{\hat{x}}_2(t) = -\beta_0(t)x_2(t) - c_0 x_1(t) + \\ &+ F_2(t) + \beta_0(t)\hat{x}_2(t) + c_0\hat{x}_1(t) - F_2(t) - \\ &- k_2(x_1(t) - \hat{x}_1(t)) = -c_0(x_1(t) - \hat{x}_1(t)) - \\ &- \beta_0(t)(x_2(t) - \hat{x}_2(t)) - k_2(x_1(t) - \hat{x}_2(t)) = \\ &- (c_0 + k_2)e_{N1}(t) - \beta_0(t)e_{N2}(t). \end{aligned}$$

Finally

$$\begin{pmatrix} \dot{e}_{N1}(t) \\ \dot{e}_{N2}(t) \end{pmatrix} = \begin{pmatrix} -k_1 & 1 \\ -(c'_0 + k_2) & -\beta_0(t) \end{pmatrix} \cdot \begin{pmatrix} e_{N1}(t) \\ e_{N2}(t) \end{pmatrix}. \quad (16)$$

The transient process  $e_N(t)$  is determined by the matrix

$$A_N(t) = \begin{pmatrix} -k_1 & 1 \\ -(c'_0 + k_2) & -\beta_0(t) \end{pmatrix}.$$

According to Demidovich stability criterion for non-stationary systems [Pavlov et al., 2004] the convergence of the system is determined by the eigenvalues of the symmetrized matrix

$$A_N(t) + A_N^T(t) = \begin{pmatrix} -2k_1 & 1 - (c'_0 + k_2) \\ 1 - (c'_0 + k_2) & -2\beta_0(t) \end{pmatrix}. \quad (17)$$

Obviously, the characteristic polynomial of the symmetrized matrix (17) is as follows

$$D(p) = p^2 + 2(k_1 + \beta_0(t))p + 4k_1\beta_0(t) - [1 - (c'_0 + k_2)]^2$$

and the discriminant of the quadratic equation reads:

$$[2(k_1 + \beta_0(t))]^2 - 4[4k_1\beta_0(t) - (1 - c_0 - k_2)^2] = 4(k_1 - \beta_0(t))^2 + 4(k_2 + c_0 - 1)^2 > 0.$$

Therefore, the equation has two real roots, which can be made negative by means of the choice of  $k_1$  and  $k_2$

$$\lambda_{1,2} = -(k_1 + \beta_0(t)) \pm \sqrt{(k_1 - \beta_0(t))^2 + (k_2 + c'_0 - 1)^2}. \quad (18)$$

Since  $\beta_0(t) \geq \beta/m_0 > 0$ , both roots are negative and uniformly separated from zero. Consequently, by the Demidovich criterion, the observation errors converge to zero. The characteristic polynomial for the observer is as follows:

$$\det(pI_2 - A_N) = \det \left( \begin{pmatrix} p & 0 \\ 0 & p \end{pmatrix} - \begin{pmatrix} -k_1 & 1 \\ -(c'_0 + k_2) & -\beta_0(t) \end{pmatrix} \right) = \det \begin{pmatrix} p + k_1 & -1 \\ c'_0 + k_2 & p + \beta_0(t) \end{pmatrix} = (p + k_1)(p + \beta_0(t)) + c'_0 + k_2 = p^2 + (k_1 + \beta_0(t))p + (k_1\beta_0(t) + c'_0 + k_2).$$

Considering that the SV-1 vibration unit coefficient coefficient  $\beta_0(t) \geq \beta/m_0 > 0$ , we can provide a predetermined set of  $A_N$  eigenvalues by choosing  $k_1$  and  $k_2$ . This ensures the specified evaluation performance.

The coefficients  $k_1, k_2$  can be chosen based on the computer simulation results from the condition that the transient time of the observation error would be 2-3 times less than the synchronization time.

## 5 Simulation Results

Efficiency of proposed observer (15) was studied in the MATLAB environment. The observer-based algorithm

$$\begin{cases} M_1 = -\gamma_1 \left\{ (1 - \alpha) (\hat{H} - H^*) \dot{\varphi}_1 + \frac{\alpha}{J_1} (\dot{\varphi}_1 \pm \dot{\varphi}_2) + \right. \\ \left. + \frac{\alpha}{J_1} (\varphi_1 \pm \varphi_2 + \Delta\varphi_1) \right\}; \end{cases} \quad (19)$$

where  $\dot{y}_c = \hat{x}_2$  is obtained from observer (15),

$$\begin{aligned} \hat{H} &= 0.5m_0\dot{y}_c^2 + 0.5J_1\dot{\varphi}_1^2 + 0.5J_2\dot{\varphi}_2^2 + \\ &+ \dot{y}_c\dot{\varphi}_1 m\varrho \cos \varphi_1 + \dot{y}_c\dot{\varphi}_2 m\varrho \cos \varphi_2 + m_0 g y_c + \\ &+ m\varrho g (\sin \varphi_1 + \sin \varphi_2) + c_{02}y_c^2, \end{aligned}$$

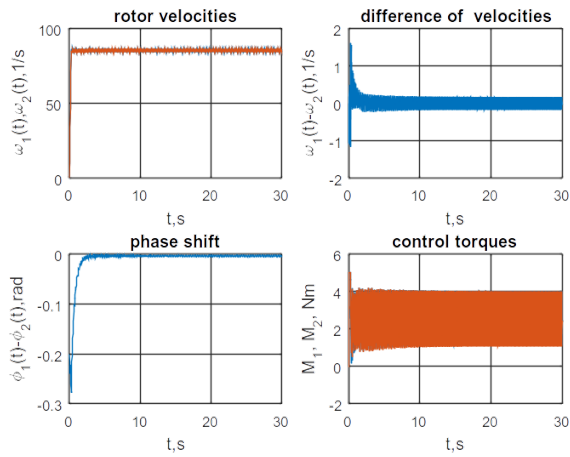


Figure 4. The dynamics of the system variables with observer.

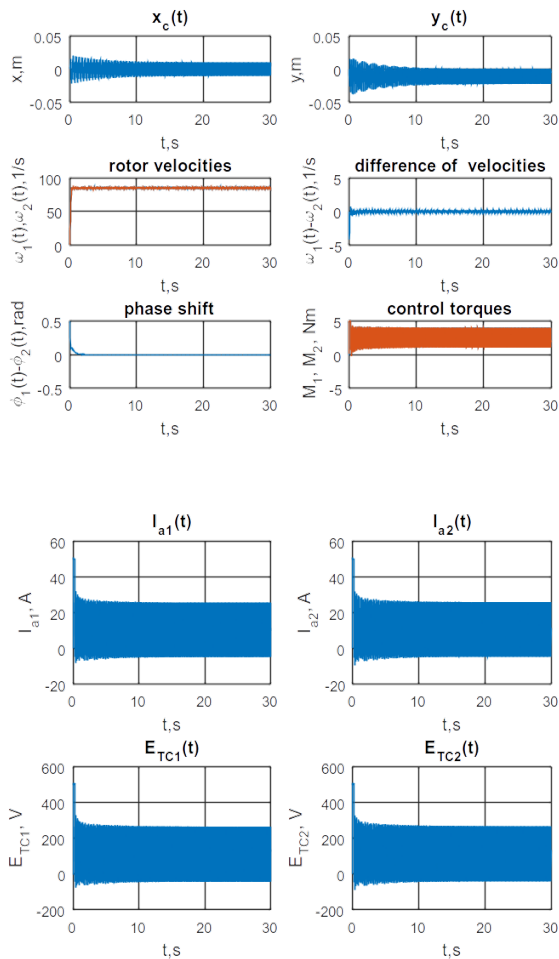


Figure 3. The dynamics of the system variables under full state measurement.

Fig. 3 corresponds to the model (1)-(2) under assumption of full state measurement with the following nominal system parameters:  $J_1 = J_2 = 0.014 \text{ kg}\cdot\text{m}^2$ ,  $J = 0.2$

$\text{kg}\cdot\text{m}^2$ ,  $m = 1.5 \text{ kg}$ ,  $m_n = 9 \text{ kg}$ ,  $\varrho = 0.04 \text{ m}$ ,  $k_c = 0.01 \text{ J/s}$ ,  $\beta = 5 \text{ kg/s}$ ,  $c_{01} = 1300 \text{ N/m}$ ,  $c_{02} = 5300 \text{ N/m}$ ,  $r = 0.2 \text{ m}$ ,  $R_a = 10\Omega$ ,  $T_a = 0.001 \text{ s}$ ,  $k_{TC} = 7.5$ ,  $T_{TC} = 0.001 \text{ s}$ ,  $b = 0.333$ ,  $\tau = 0.001 \text{ s}$ ,  $ku = 10 \frac{1}{\sqrt{s}}$ .

The dynamics of the following variables are presented in Fig. 3: the horizontal and vertical displacements of the supporting body  $x_c, y_c$ , rotor velocities  $\dot{\varphi}_1, \dot{\varphi}_2$ , difference of velocities  $\dot{\varphi}_1 - \dot{\varphi}_2$ , phase shift  $\varphi_1 - \varphi_2$ , controlling torques  $M_1, M_2$ , the armature currents  $I_{a1}, I_{a2}$ , converter EMFs  $E_{TC1}, E_{TC2}$ .

In Fig. 4 the plots for the variables ( $\dot{\varphi}_1, \dot{\varphi}_2, \dot{\varphi}_1 - \dot{\varphi}_2, \varphi_1 - \varphi_2, M_1, M_2$ ), where the controlling torques  $M_1, M_2$  are evaluated based on the observer estimates (19) for  $k_1 = 100, k_2 = 1000$  are shown. As seen from the plots the values of synchronization time, transient time for rotor velocities, as well as the magnitude values  $|y(t)_{\max}|$ , and  $\max |\dot{\varphi}_1 - \dot{\varphi}_2|$  do not exceed those for full state measurement case.

From the equations of the non-stationary observer, it is clear that an important issue is the question of choosing the gains  $k_1$  and  $k_2$ . These coefficients are selected using computer simulation in such a way that the maximum values of observation errors for both variables are minimal in magnitude. The quantitative characteristics of this study are shown in Table 1. The graphs of observer errors  $e_{N1}$  and  $e_{N2}$  are shown in Fig. 5 and Fig. 6. As can be seen from the table, the best results were obtained with the values of the gains  $k_1 = 100, k_2 = 1000$  ( $e_{N1} = 1 \cdot 10^{-4} \text{ m}$ ,  $e_{N2} = 0.01 \text{ m/s}$ ). It should be noted that, in addition to the fact that good estimation indicators are obtained for large values of the gains  $k_1$  and  $k_2$ , the relationship between these coefficients is also important. E.g. for  $k_1 = 10, k_2 = 10000$  the processes are the worst in terms of observation errors.

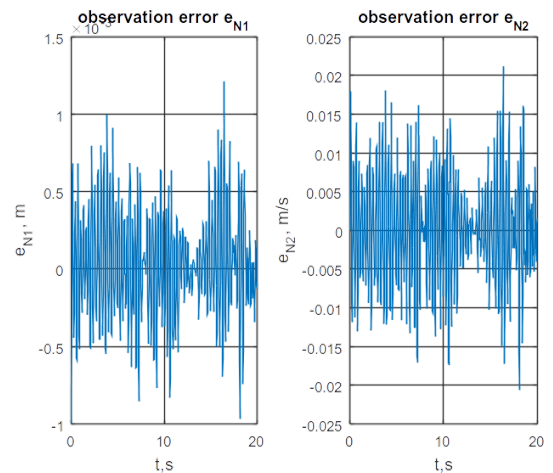


Figure 5. The graphs of observation errors for  $k_1 = 1, k_2 = 10$ .

In Fig. 5 and Fig. 6 the graphs of observation errors  $e_{N1}, e_{N2}$  for two different observer gain values are

Table 1.

Observer gains		Magnitude of observation errors	
$k_1$	$k_2$	$e_{N1}, m$	$e_{N2}, m/s$
1	10	$1 \cdot 10^{-3}$	0.02
1	100	$1.1 \cdot 10^{-3}$	0.025
10	100	$4 \cdot 10^{-4}$	0.01
10	1000	$6 \cdot 10^{-3}$	0.03
10	10000	$9 \cdot 10^{-3}$	0.1
100	100	$5 \cdot 10^{-4}$	0.02
100	1000	$1 \cdot 10^{-4}$	0.01

shown:  $k_1 = 1, k_2 = 10$  and  $k_1 = 100, k_2 = 1000$  respectively. As seen from the graphs, the normalized observation error for the velocity of the supporting body is as follows

$$E = \frac{\max |e_{N2}|}{\max |dy_c/dt|} \cdot 100\% = 2.5\%.$$

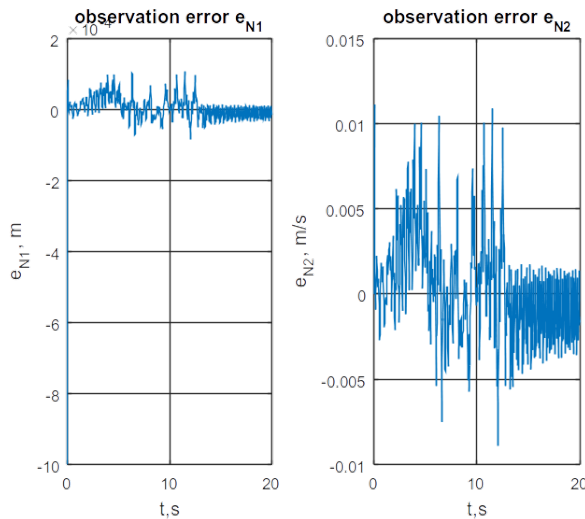


Figure 6. The graphs of observation errors for  $k_1 = 100, k_2 = 1000$ .

## Conclusion

In this paper the control of oscillations in the two-rotor vibration unit is studied. It is assumed that the velocity of the oscillation of the platform cannot be accurately measured. The time-varying observer is proposed to restore it. The synthesis of the observer is performed according to a simplified model of the dynamics of a two-rotor vibration unit describing the movement of the installation

along the vertical axis Oy In order to guarantee stability of the frequency and amplitude of oscillations of the vibrating parts of a two-rotor vibration unit special control algorithms based on speed-gradient methodology. Simulation results confirm stability of the synchronous rotation modes of the unbalanced rotors of the vibration unit.

Further research is aimed at the study of the influence of the communication delay occurring e.g. when controlling via Internet. It is expected that in this case, the use of an observer which is to some extent a smoothing filter can improve the quality of the control signal and reduce the signal distortion.

## References

- Andrievskii, B.R., Blekhman, I.I., Bortsov, Yu.A., Gavrilov, S.V., Konoplev, V.A., Lavrov, B.P., Polyakhov, N.D., Tomchina, O.P., Fradkov, A.L., et al., (2001). *Upravlenie Mekhatronnymi Vibratsionnymi Ustanovkami (Control of Mechatronic Vibrational Units)*, Blekhman, I.I. and Fradkov, A.L., Eds., St. Petersburg: Nauka.
- Blekhman, I.I. (2000). *Vibrational Mechanics: Nonlinear Dynamic Effects, General Approach, Applications*. World Scientific.
- Blekhman, I.I., Fradkov, A.L., Tomchina, O.P., and Bogdanov, D.E. (2002). Self-synchronization and controlled synchronization: general definition and example design. *Mathematics and Computers in Simulation*, **58**:4–6, pp.367–384.
- Bobtsov, A. A., Pyrkin, A. A., Ortega, R.S. et al. (2018). A state observer for sensorless control of magnetic levitation systems. *Automatica*, **97**: 11, pp. 263–270.
- Efimov, D., Fradkov, A.L., and Iwasaki, T. (2013). Exciting multi-DOF systems by feedback resonance. *Automatica*, **49**:6, pp. 1782–1789.
- Fradkov, A.L., Miroshnik, I.V., and Nikiforov, V.O. (1999). *Nonlinear and Adaptive Control of Complex Systems*. Dordrecht: Kluwer, Academic Publ. 510 p.
- Fradkov, A.L. (1999). Exploring nonlinearity by feedback. *Physica D*, **128**, pp.159–168.
- Fradkov, A.L., Tomchina, O.P., Galitskaya, V.A., and Gorlatov, D.V. (2013). Integrodifferentiating speed-gradient algorithms for multiple synchronization of vibration units. *Nauchno-tehnicheskii Vestnik of ITMO*, St.Petersburg, No. 1, pp. 30–37.
- Fradkov, A.L., Tomchina, O.P., Tomchin, D.A., and Gorlatov, D.V. (2016). Time-varying observer of the supporting body velocity for vibration units. *IFAC 6-th IFAC Workshop on Periodic Control Systems, PSYCO*, **49**: 14, pp. 18–23.
- Lascu, C., Boldea, I., and Blaabjerg, F. (2000). A modified direct torque control for induction motor sensorless drive. *IEEE Transactions on industry applications*, **36**: 1, pp. 122–130.

- Ortega, R., Sarr, A., Bobtsov, A., Bahri, I., and Diallo, D. (2019). Adaptive state observers for sensorless control of switched reluctance motors. *International Journal Of Robust And Nonlinear Control*, **29**: 4, pp. 990–1006.
- Pavlov, A., Pogromsky, A., van de Wouw, N., and Nijmeijer, H. (2004). Convergent dynamics, a tribute to Boris Pavlovich Demidovich. *Systems & Control Letters* **52**, pp. 257–261.
- Tomchina, O. (2018). Control of vibrational field in a cyber-physical vibration unit. *Cybernetics And Physics*, **7**:3, pp. 144–151.
- Tomchina, O. (2019). Control of vibrational field in a vibration unit: influence of drive dynamics. *Cybernetics And Physics*, **8**: 4, pp. 298–306.
- Tomchina, O.P., Gorlatov, D.V., and Tomchin, D.A. (2015). Controlled passage through resonance for two-rotor vibration unit: Influence of drive dynamics. *IFAC-PapersOnline*, **48**: 11, pp. 313–318.
- Wang, Qiong, Wang, Shuanghong, Chen, Chuanhai (2019). Review of sensorless control techniques for PMSM. *IEEE Transactions on electrical and electronic engineering*, **14**: 10, pp. 1543–1552.